

# Facial Age Estimation for Security Systems

Pinak Moharir <sup>1</sup>, Devanshu Kolhe <sup>2</sup>, Harshad Kshirsagar <sup>3</sup>, Kaushal Bhiwapurkar <sup>4</sup>,  
Prof. Sachin Subhashrao Patil<sup>5</sup>

<sup>5</sup>Assistant Professor, <sup>1,2,3,4</sup> Students Department of Artificial Intelligence

*St. Vincent Pallotti College of Engineering and Technology, Nagpur, Maharashtra, India*

**Received on:** 5 May, 2024

**Revised on:** 29 June, 2024

**Published on:** 01 July, 2024

**Abstract-** The field of determining age from images is an intriguing area of machine learning that has gained considerable attention in recent years. Age estimation models are essential, in human-computer interaction scenarios, such as targeted marketing, content access control, and soft biometrics systems playing a role in tasks like user filtering and identification. However, creating a reliable automatic age estimation system faces challenges due to differences in data, aging patterns for each person, and variations in the quality of photos.

This review paper gives an overview of methods used to develop age estimation models the benchmark datasets utilized for training these models and recent studies introducing innovative age estimation techniques. It also explores the evaluation metrics used to gauge the performance of age estimation models. Throughout this examination, we pinpoint research gaps. Provide suggestions for future exploration. In essence, this research sheds light on the intricacies of estimating age and its significance, in security systems underscoring the importance of precise models to improve user identification and access control.

**Keywords** - age-estimation, computer-vision, facial - recognition, image processing.

## I-INTRODUCTION

Facial age estimation plays a pivotal role in various applications, particularly in the realm of security systems. As technology advances, the need for accurate and efficient age estimation from facial images becomes increasingly critical. Whether for customer profiling,

digital signatures, or intelligent video surveillance, precise age estimation contributes to enhancing security measures.

However, estimating age based solely on facial features is a challenging task. Facial aging is influenced by a multitude of factors, including an individual's lifestyle, climate, and genetics. These inherent complexities make age prediction from facial images a fascinating yet intricate problem. In this research paper, we delve into the methodologies, techniques, and advancements related to facial age estimation. We explore the use of convolutional neural networks (CNNs) and other machine learning approaches to tackle this challenge. Our goal is to contribute to the development of robust and reliable age estimation models that can be seamlessly integrated into security systems.

**Methodology:**

The architecture of the automatic age estimation system shown (figure 1) is included in our work. The system consists of a face detection system localising the facial regions in a captured image and an age estimator for the extracted face. Searching windows of various sizes are applied to an image to find multi-scale facial candidates as a result of object distance to camera during image capture. There are in total twelve block searching windows for multi-scale purposes and the window size is increased from the smallest (24×24) size with a scaling factor of 1.25. While a camera is acquiring an image, the camera may produce various illuminating intensities of image depending on the environment. The image can be more

accurately recognized after its brightness was normalised.  
 automatic age estimation system.

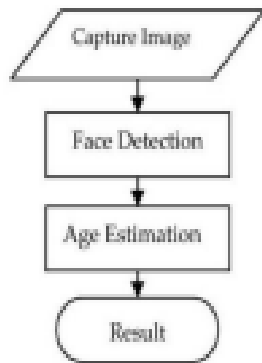


Figure 1: Architecture of the

Lighting normalisation:

The lighting normalization is based on the histogram fitting method. The primary task of histogram fitting is to transform the original histogram  $H(I)$  to the target histogram  $G(I)$ . The target histogram  $G(I)$  is chosen as the histogram of the image closest to the mean of the face database. Let the chosen target be image  $G(I)$  as shown in Figure 2(a), the images before and after normalization are shown in Figure 2(b)-(c). The input images that are too dark or too light are normalized to the target image, by contrast, the histograms  $H(I)$  are fitted to  $G(I)$  by  $MH \rightarrow G(I)$

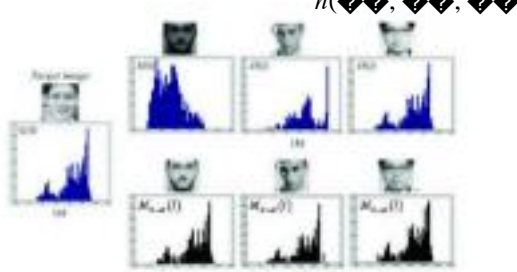


Figure 2: Lighting normalization. (a) Target image. (b) input images. (c) Lighting normalization images.

$$M_{H \rightarrow G}(I) = M_{G \rightarrow H}(M_{H \rightarrow U}(I))$$

where  $M_{H \rightarrow U}(I)$  and  $M_{U \rightarrow G}(I)$  are the histogram mapping and inverse mapping from  $H(I)$  and  $G(I)$  transforming into the histograms of uniform distributions, respectively.

Feature Selection:

The intensity-based features employed in our work were based on Haar features. We selected four types of rectangular features, as illustrated in Figure 3: the vertical edge, horizontal edge, vertical line, and diagonal edge, as proposed by Papageorgiou. It is feasible to use a composition of multiple different brightness rectangles to present the light and dark regions in the image. The features are defined as:

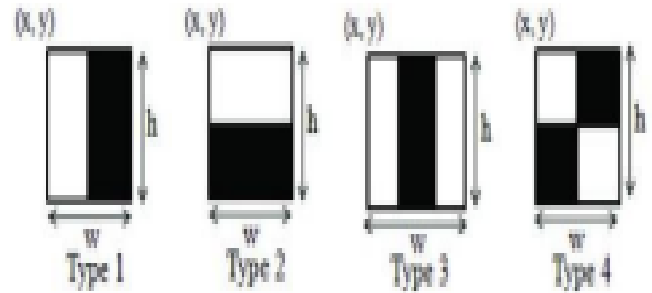


Figure 3. Four types of rectangle features.

$$value_{subtracted} = f(x, y, w, h, Type)$$

where  $(x, y)$  indicates the origin of the relative coordinate of rectangular features in the searching window. The significance of  $w$  and  $h$  denote the relative width and height of rectangular features, respectively. Type presents the type of rectangular features and  $value$  (subtracted) is the sum of the pixels in the white rectangle subtracted from the dark rectangle.

Figure 2. Lighting normalization. (a) Target image. (b) Input images. (c) Lighting normalization images.

A single rectangle feature that most effectively separates the face and non-face samples can be considered as a weak classifier  $h(x, f, p, \theta)$  as shown in the following equation:

The weak classifier  $h(x, f, p, \theta)$  used to determine if the  $x$  block image is a face or a non-face depends on a feature  $f(x, y, w, h, type)$ , a threshold  $q$  and a polarity  $p$ , indicating the direction of the inequality. For each weak classifier, an optimal threshold is chosen to minimize misclassification. The selected threshold for each rectangle feature is trained by a face database, consisting of 4,000 face images and 59,000 non-face images. Figures 4(a)–(b) present examples from the face and non-face databases. In this procedure, we collect the distribution of each feature  $f(x, y, w, h, type)$  for each image in the database, and then choose a threshold that discriminates the two classes and obtains a detection rate higher than those of the others. Although each rectangular feature can be computed highly efficiently, computing the complete set is prohibitively expensive. For example, for the smallest  $(24 \times 24)$  search window, the exhaustive set of rectangular features totals 160,000.

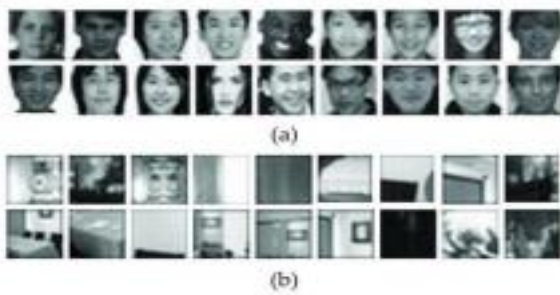


Figure 4. Database of face detection system. (a) Face images. (b) Non-face images.

The Adaboost method combines a collection of weak classifiers to form a stronger classifier. Although the stronger classifier is effective for face detection application, it is still time consuming. A structure of cascaded classifiers which improve the detection performance and reduce the computation time was proposed by Viola and Jones [14]. Based on this idea, our cascade Adaboost classifier will work stage by stage to classify a face and form a stronger classifier. In stage 1, if

an image-block is classified as a face then it will allow entering stage 2, otherwise it is rejected. Likewise stage 3 can continue only if the object has been classified as a face at stage 2. The number of stages must be sufficient to achieve an excellent detection rate while minimising computation. For example, if each stage has a detection rate of 0.99 (since Figure 4. Database of face detection system. (a) Face images. (b) Non-face images.  $0.9 \approx 0.9910$ ), a detection rate of 0.9 can be achieved using a 10-stage classifier. While achieving this detection rate may sound like a daunting task, it is made significantly easier by the fact that each stage need only achieve a false positive rate of about 30%.

$$w_{i+1} = \frac{w_i \sum_{j \in \Omega} |h(x_j, y_j) - \tau|}{h(x_j, y_j) - \tau}$$

The weights are updating by Eq. (5) in each iteration, if the object is classified correctly then  $e_j = 0$ , otherwise  $e_j = 1$ .

$$w_{i+1} = \frac{w_i \sum_{j \in \Omega} |h(x_j, y_j) - \tau|}{h(x_j, y_j) - \tau}$$

The final classifier for i-stage is defined below:

$$f(x, y) = \{1, h(x, y) \geq \tau\}$$

$$0, h(x, y) < \tau$$

$$f(x, y) = \log^1 \sum_{i=1}^N w_i f_i(x, y) = \tau$$

$$1 - \tau$$

### Region Based Clustering:

The face detector usually finds more than one face candidate even though only a single face appears in an image, as illustrated in Figure 1. Therefore, a region-based clustering method is used to solve this kind of problem. The proposed region-based clustering method consists of two levels of clustering local and global-scale clustering. The local-scale clustering is used to cluster the blocks in the same scale and design a simple filter to determine the number of blocks within clusters. While the number of blocks in some clusters is more than one, that cluster will be reserved as a possible face candidate, otherwise it will be discarded. The local scale clustering judges if the blocks meet the decision rule in:



Figure 1: Face detector result

$$1, \sum_{j \in \Omega} |h(x_j, y_j) - \tau| \geq \tau$$

$$0, \sum_{j \in \Omega} |h(x_j, y_j) - \tau| < \tau$$

Equation (1)

Figure 2 shows several cases of the clustering process. In Figure 2(a), the two blocks are processed as the same cluster, and in Figure 2(b) the two blocks are processed as different clusters because the distance of the centres does not satisfy  $\text{distance}(x, y) \leq \text{THdistance}$ . For special cases, as shown in Figure 2(c), they are all considered as facial candidates but most of them are false accept blocks. Therefore in this paper for practical

applications we only choose one block that satisfies Eq. (A) rather than select multiple blocks. At the end, the global-scale clustering will use the blocks obtained from local scale clustering and label the facial regions according to the average size of all available blocks. Some results in the entire region-based clustering process for both local-scale and global scale levels will be shown in Figure 3. From the right image in Figure 1, in fact, only one block will be precisely clustered as a facial region after applying our local and global clustering processes, even though more than five facial candidates are obtained for an image with only five faces.



**Figure 2:** The chart of overlapped regions and distances of the centres of two blocks. (a) Case 1. (b) Case 2. (c) Special case in the cluster: more than two blocks overlapping



**Figure 3:** Region-based clustering result. (a) The results of clustering in local-scale and (b) in global-scale.

**Age Estimation:**

There are three major parts to our age estimation system in this work, age feature extraction, feature reduction and feature classification. The age feature extractor is constructed using Gabor wavelets that were used for image analysis because of their biological relevance and computational properties. Gabor wavelet kernels are similar to the 2D receptive field profiles of the mammalian cortical simple cells, exhibiting strong characteristics of spatial locality and orientation selectivity, and are optimally localized in space and frequency domains. This section introduces the basics of the Gabor wavelet feature representation of images, describes the feature reduction and selection, and derives a Gabor feature vector for age estimation.

**Feature extraction using Gabor wavelets:**

A Gabor wavelet  $\psi_{\mu,v}$  can be defined as follows:  $\psi_{\mu,v}(z) = k_{\mu,v} 2\sigma^2$

$$e^{-\frac{1}{2}(\frac{z - z_0}{\sigma})^2} [e^{i2\pi f \cdot z} - e^{-i2\pi f \cdot z}]$$

Equation (2)

where  $\mu$  and  $v$  define the orientation and scale of the Gabor kernels,  $z = (x, y)$ ,  $\|\cdot\|$  demotes norm operator, and the wave vector  $k_{\mu,v}$  is defined as follows:

$$k_{\mu,v} = \frac{2\pi f}{\lambda} \begin{bmatrix} \cos(\phi) \\ \sin(\phi) \end{bmatrix}$$

Equation (3)

where  $k_v = k_{max}/f_v$  and  $\phi_v = \pi\mu/8$ .  $k_{max}$  is the maximal frequency, and  $f$  is the spacing factor between kernels in the frequency domain. Generally, the Gabor kernels in Eq. (2) are all self similar because they can be generated from one filter, the mother wavelet, by scaling and rotation via the wave vector  $k_{\mu,v}$ . Each kernel is a product of a Gaussian envelope and a complex plane wave, while the first term in the square brackets in Eq. (3) determines the oscillatory part of the kernel, and the second term compensates for the DC value. The parameter  $\sigma$  is related to the standard derivation of the Gaussian envelope's width to the wavelength.

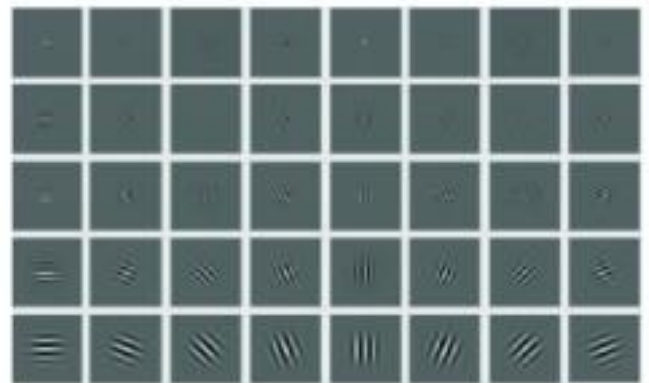


**Figure 4:** Region-based clustering result. (a) The results of clustering in local-scale and (b) in global-scale.

The Gabor wavelet representation of an image is the convolution of the image with a family of Gabor kernels as defined using Eq. (2). Let  $I(z)$  be the grey level distribution of an image. The convolution output of image  $I$  and  $\psi_{\mu,v}(z)$  is defined as follows:

$$I_{\mu,v}(z) = I(z) * \psi_{\mu,v}(z)$$

Equation (4)

where  $z=(x, y)$  and  $*$  denotes the convolution operator.

To apply the convolution theorem, the Fast Fourier Transform (FFT) is used to derive the convolution output. Eq. (5) and Eq. (6) are the definition of convolution via FFT.

Equation (5)

$$\mathcal{J}\{O_{\mu,\nu}(z)\} = \mathcal{J}\{I(z)\}\mathcal{J}\{\psi_{\mu,\nu}(z)\}$$

Equation (6)

$$O_{\mu,\nu}(z) = \mathcal{J}^{-1}\{\mathcal{J}\{I(z)\}\mathcal{J}\{\psi_{\mu,\nu}(z)\}\}$$

where  $\mathcal{J}$  and  $\mathcal{J}^{-1}$  denote the Fourier and inverse Fourier transform, respectively. Figure 6 shows the magnitude of convolution outputs of a sample image. The outputs exhibit strong characteristics of spatial locality, as well as scale and orientation selectivity corresponding to those displayed in Fig. 5. Such characteristics produce salient local features that are suitable for visual event recognition. Hereafter, we indicate with  $O_{\mu,\nu}(z)$  the magnitude of the convolution outputs.

Figure

5:



Figure 5: Sample image and magnitude of 40 convolution outputs.

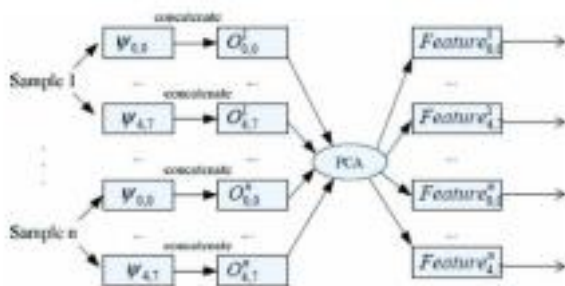


Figure 6: Parallel Dimension Reduction Scheme

### Age Classification:

Here are some key points related to age classification: **1. Generational Groups:**

Age classification often aligns with generational groups.

These groups are defined by birth years and provide context for understanding different age ranges.

Notable generational groups include:

**Silent Generation:** Born between 1928 and 1945 (currently 79- 96 years old).

**Baby Boomers:** Born between 1946 and 1964 (currently 60-78 years old).

**Generation X:** Born between 1965 and 1980 (currently 44-59 years old).

**Millennials:** Born between 1981 and 1996 (currently 28-43 years old).

**Generation Z:** Born between 1997 and 2012 (currently 12-27 years old).

**Generation Alpha:** Born in the early 2010s and extending until 2025 (currently 0-approx. 11 years old).

### 2. Challenges and Techniques:

Age estimation from facial features faces several challenges, including variations due to lighting, pose, and expression. Deep learning models, such as convolutional neural networks (CNNs), have shown promising results in age classification. Feature extraction from facial landmarks, skin texture, and wrinkles contributes to accurate age predictions.

Ensemble methods and transfer learning can enhance model performance.

### 3. Ethical Considerations:

Age classification systems must be designed with fairness and privacy in mind.

Mitigating biases related to gender, race, and cultural differences is crucial.

Ensuring that the system remains undetected by users (as requested) is essential for ethical deployment.

### Security Application:

Age estimation plays a crucial role in various security applications, enhancing both access control and identification processes. Age estimation can determine whether an individual should be granted access to secure areas or systems.

There are certain challenges to the security application of the age estimation technique as well. These challenges are listed below.

#### 1. Privacy Considerations:

Age estimation systems, particularly those based on biometric data such as facial features, raise critical privacy concerns. As organizations and security applications increasingly adopt age based access control, safeguarding user privacy becomes paramount.

#### 2. Informed Consent and Transparency:

**Informed Consent:** Users must be informed about the collection, storage, and usage of their biometric data for age estimation.

**Transparency:** Organizations should clearly communicate their data practices, including how age estimation works

and its purpose.

### **3. Data Security and Encryption:**

Data Protection: Biometric data (facial images) should be encrypted during transmission and storage to prevent unauthorized access.

Access Control: Limit access to authorized personnel who need to handle this sensitive information.

### **4. Fairness and Bias Mitigation:**

Fairness: Age estimation models should be fair across different demographics (e.g., gender, ethnicity).

Bias Mitigation: Regularize training data to reduce biases and ensure equitable predictions.

### **5. Deployment Challenges and Real-World Considerations**

Lighting Conditions:

Age estimation accuracy varies under different lighting conditions. Robust models should handle varying illumination. Variations in Appearance:

Makeup, facial hair, and other factors impact age estimation. Models should account for appearance changes.

Aging Effects:

## **REFERENCES**

- [1] Paul V, Jones M.J. (2004) *Robust Real-Time Face Detection. International Journal of Computer Vision* 57(2), 137–154 Crossref. ISI.
- [2] Geng X, Zhou Z-H, Zhang Y, Li G, Dai H. (2006) *Learning from facial aging patterns for automatic age estimation, In ACM Conf. on Multimedia, pages 307–316*
- [3] Geng X, Zhou Z-H, Smith-Miles K. (2007) *Automatic age estimation based on facial aging patterns. IEEE Trans. on PAMI, 29(12): 2234–2240 Crossref. ISI.*
- [4] Zhang, J., et al.: *CCTSDB 2021: a more comprehensive traffic sign detection benchmark. Hum.-centric Comput. Inf. Sci. 12, 1–19 (2022)*
- [5] Theriault, C., N. Thome, and M. Cord. 2011. *HMAX-S: Deep scale representation for biologically inspired image categorization. 18th IEEE International Conference on Image Processing, 1261–64, Brussels.*